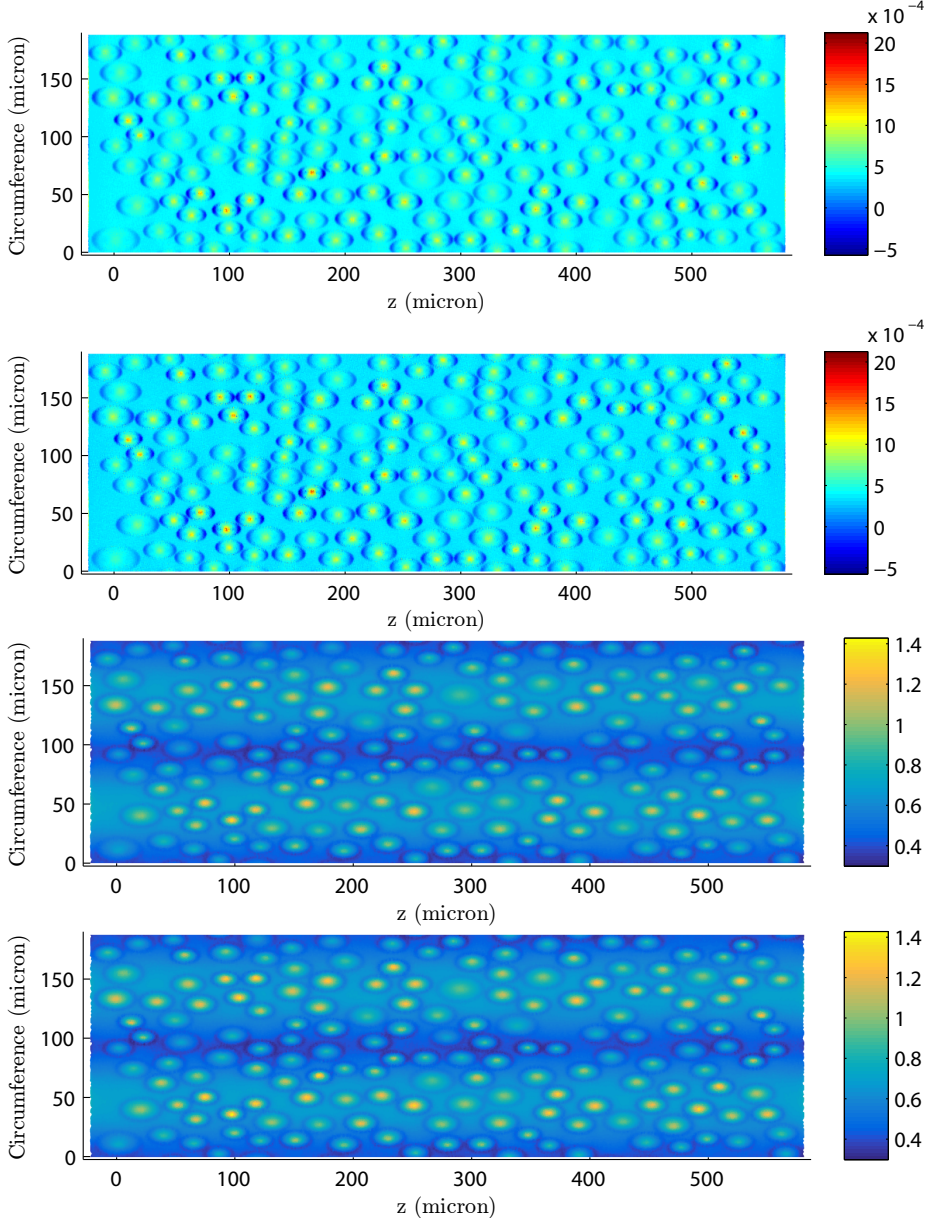
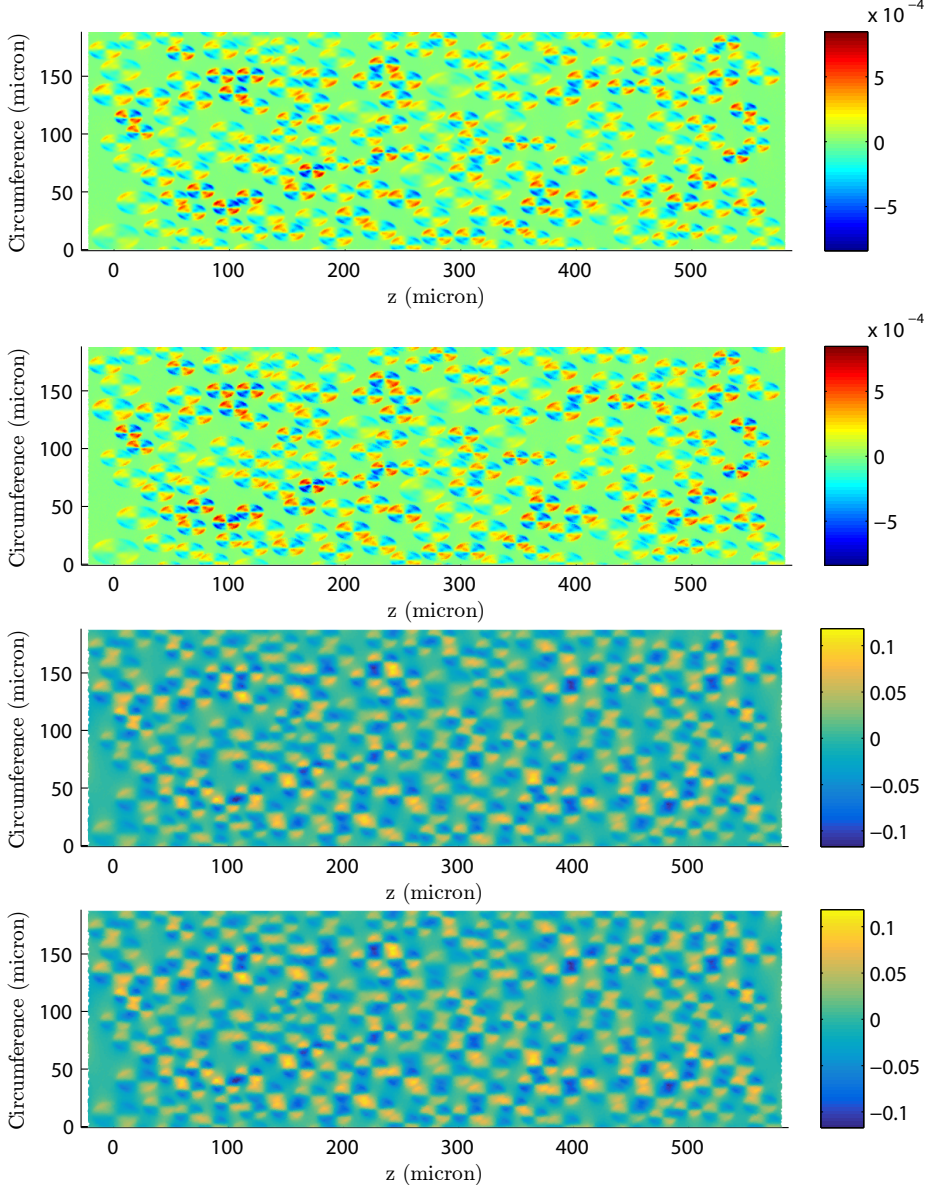


**Supplementary Material***Single-Layer Stokes Model Results*

In this supplementary material, we have included additional plots of the shear stress experienced by the endothelium for the single-layer Stokes model which were omitted from the paper for brevity.



**Figure 1:** Longitudinal component of (a,b) fluid shear stress,  $g_z$ , and (c,d) elastic shear stress,  $h_z$ , exerted upon the endothelium in the low permeability limit ( $K_P = 10^{-12} \text{ cm}^2$ ,  $\lambda = 10^{3.5}$ ) when the minimum EGL thickness is  $t_{\min} = 0.25$ ,  $\alpha_0 = 1.8$ . These stresses are computed using the asymptotic expression (3.10) and (3.27)-(3.29), respectively. We consider both a redistributed EGL of varying thickness (Model A, top image), and a non-redistributed EGL (Model B, bottom image)



**Figure 2:** Azimuthal component of (a,b) fluid shear stress,  $g_\theta$ , and (c,d) elastic shear stress,  $h_\theta$ , exerted upon the endothelium in the low permeability limit ( $K_P = 10^{-12} \text{ cm}^2$ ,  $\lambda = 10^{3.5}$ ) when the minimum EGL thickness is  $t_{\min} = 0.25$ ,  $\alpha_0 = 1.8$ . These stresses are computed using the asymptotic expression (3.10) and (3.27)-(3.29), respectively. We consider both a redistributed EGL of varying thickness (Model A, top image), and a non-redistributed EGL (Model B, bottom image)

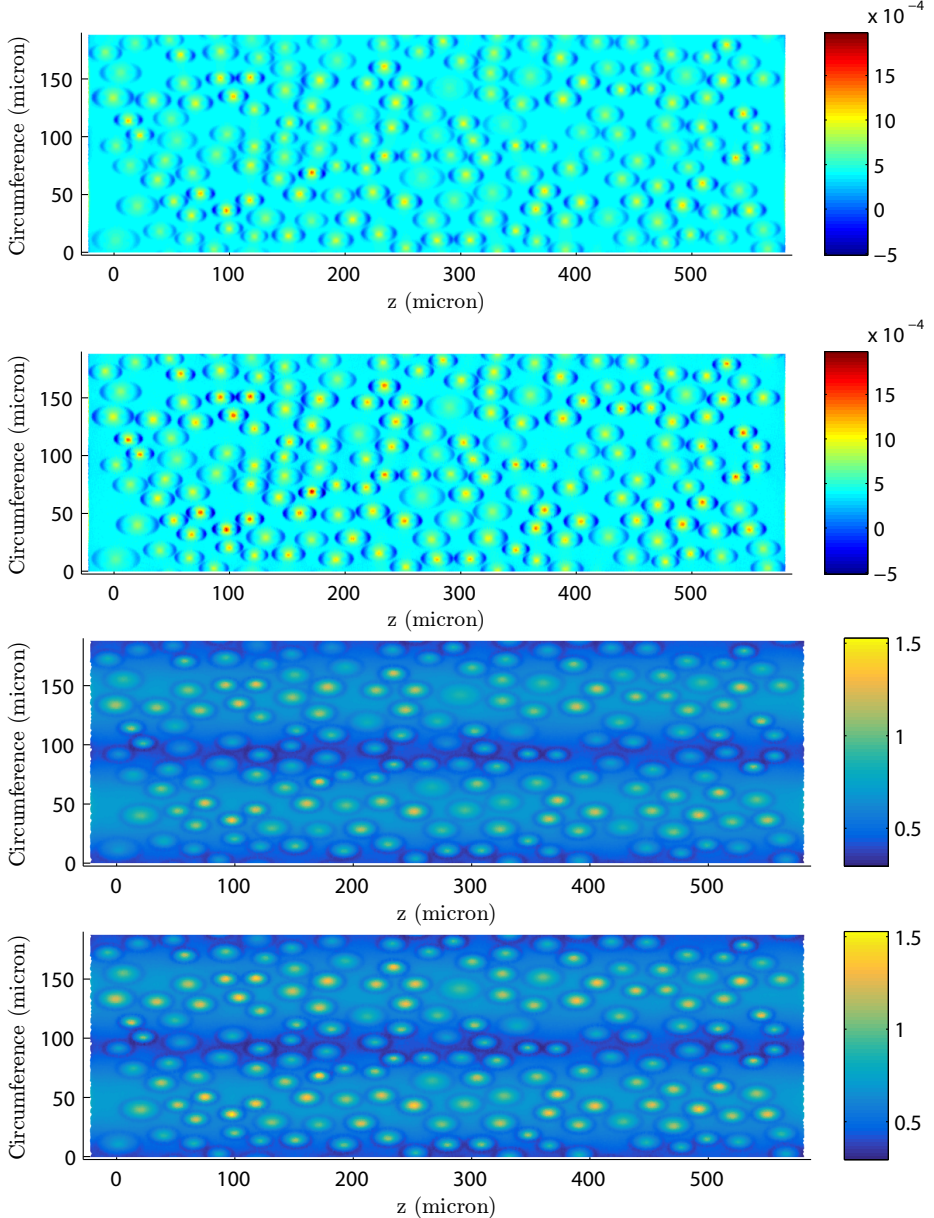


**Figure 3:** Longitudinal component of (a,b) fluid shear stress,  $g_z$ , and (c,d) elastic shear stress,  $h_z$ , exerted upon the endothelium in the low permeability limit ( $K_P = 10^{-12} \text{ cm}^2$ ,  $\lambda = 10^{3.5}$ ) when the minimum EGL thickness is  $t_{\min} = 0.5$ ,  $\alpha_0 = 1.8$ . These stresses are computed using the asymptotic expression (3.10) and (3.27)-(3.29), respectively. We consider both a redistributed EGL of varying thickness (Model A, top image), and a non-redistributed EGL (Model B, bottom image)

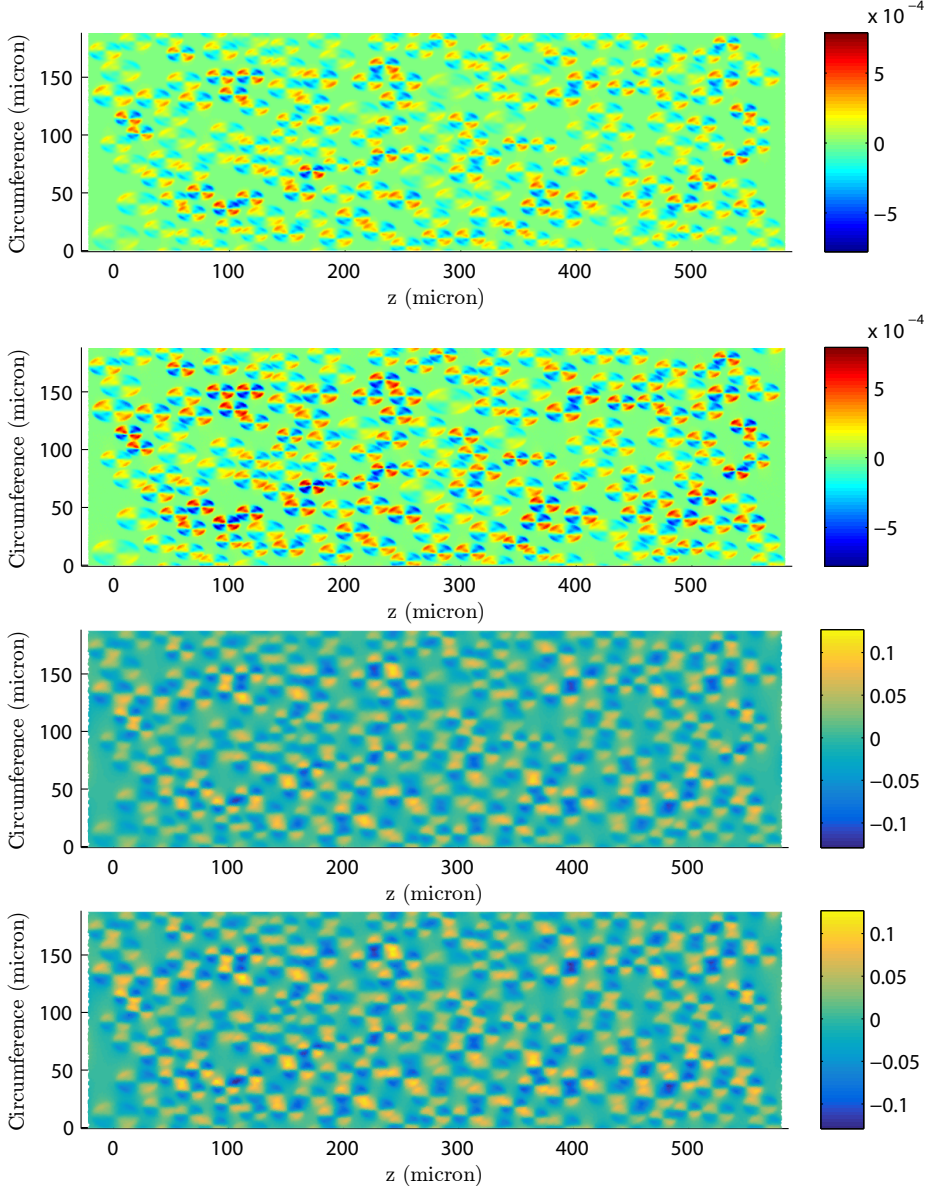


**Figure 4:** Azimuthal component of (a,b) fluid shear stress,  $g_\theta$ , and (c,d) elastic shear stress,  $h_\theta$ , exerted upon the endothelium in the low permeability limit ( $K_P = 10^{-12} \text{ cm}^2$ ,  $\lambda = 10^{3.5}$ ) when the minimum EGL thickness is  $t_{\min} = 0.5$ ,  $\alpha_0 = 1.8$ . These stresses are computed using the asymptotic expression (3.10) and (3.27)-(3.29), respectively. We consider both a redistributed EGL of varying thickness (Model A, top image), and a non-redistributed EGL (Model B, bottom image)

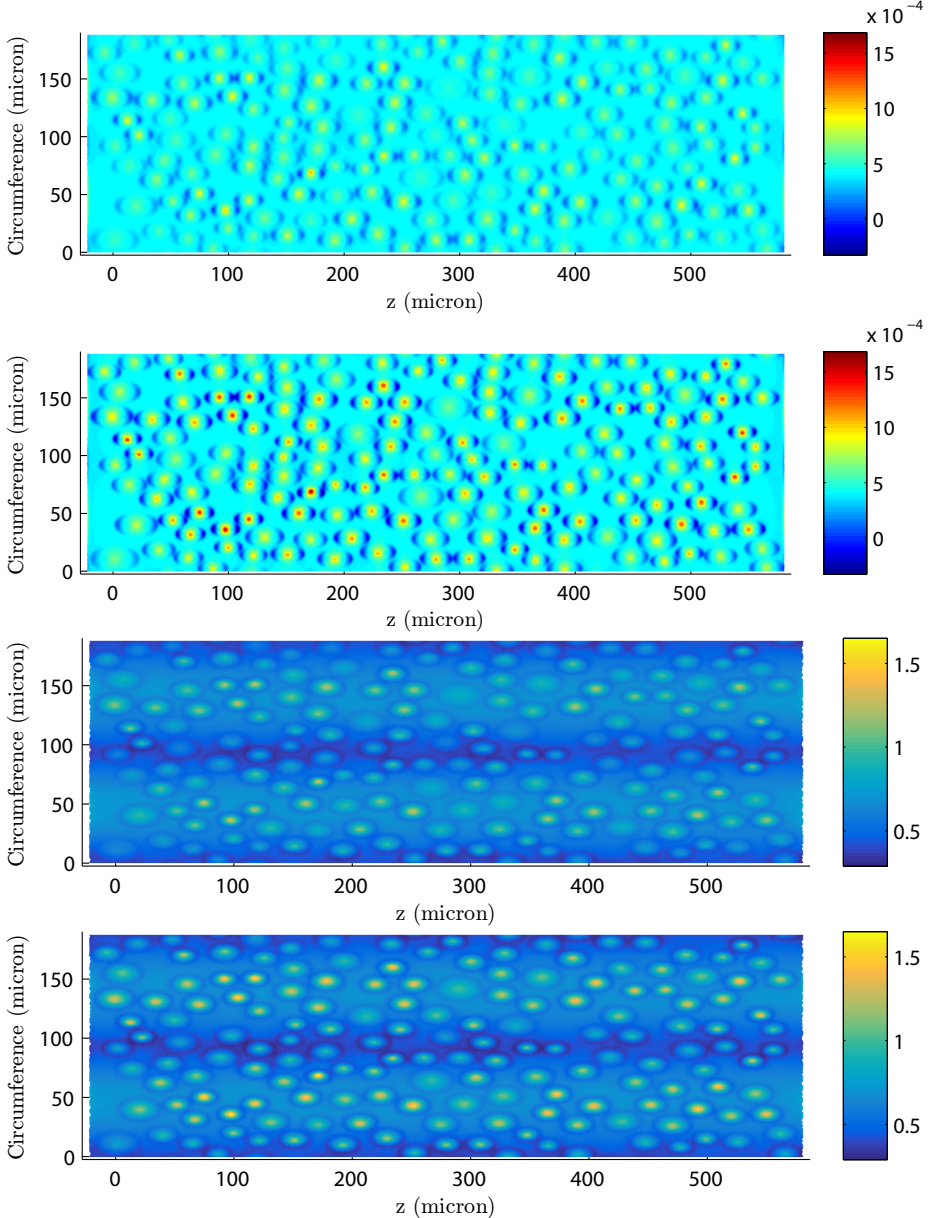


**Figure 5:** Longitudinal component of (a,b) fluid shear stress,  $g_z$ , and (c,d) elastic shear stress,  $h_z$ , exerted upon the endothelium in the low permeability limit ( $K_P = 10^{-12} \text{ cm}^2$ ,  $\lambda = 10^{3.5}$ ) when the minimum EGL thickness is  $t_{\min} = 1$ ,  $\alpha_0 = 1.8$ . These stresses are computed using the asymptotic expression (3.10) and (3.27)-(3.29), respectively. We consider both a redistributed EGL of varying thickness (Model A, top image), and a non-redistributed EGL (Model B, bottom image)

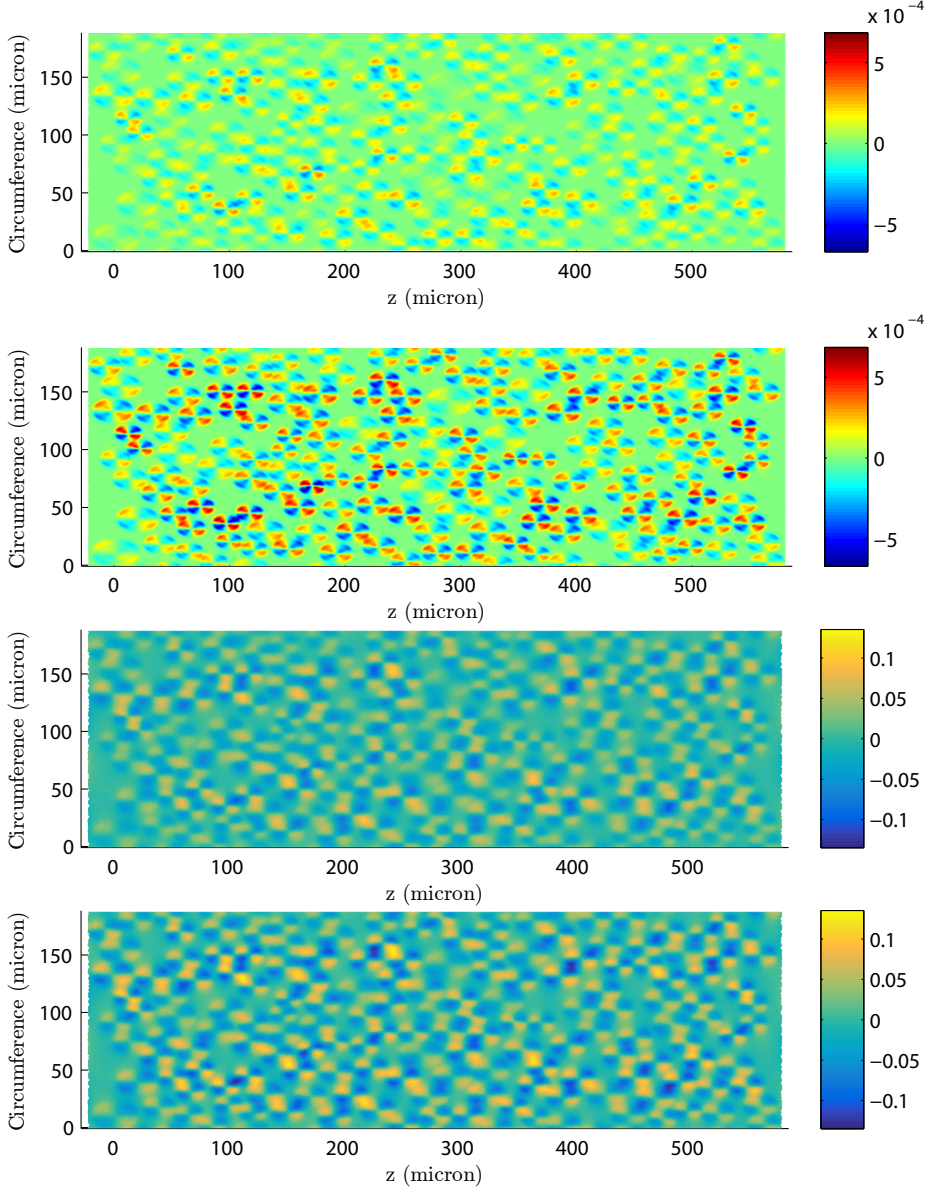


**Figure 6:** Azimuthal component of (a,b) fluid shear stress,  $g_\theta$ , and (c,d) elastic shear stress,  $h_\theta$ , exerted upon the endothelium in the low permeability limit ( $K_P = 10^{-12} \text{ cm}^2$ ,  $\lambda = 10^{3.5}$ ) when the minimum EGL thickness is  $t_{\min} = 1$ ,  $\alpha_0 = 1.8$ . These stresses are computed using the asymptotic expression (3.10) and (3.27)-(3.29), respectively. We consider both a redistributed EGL of varying thickness (Model A, top image), and a non-redistributed EGL (Model B, bottom image)

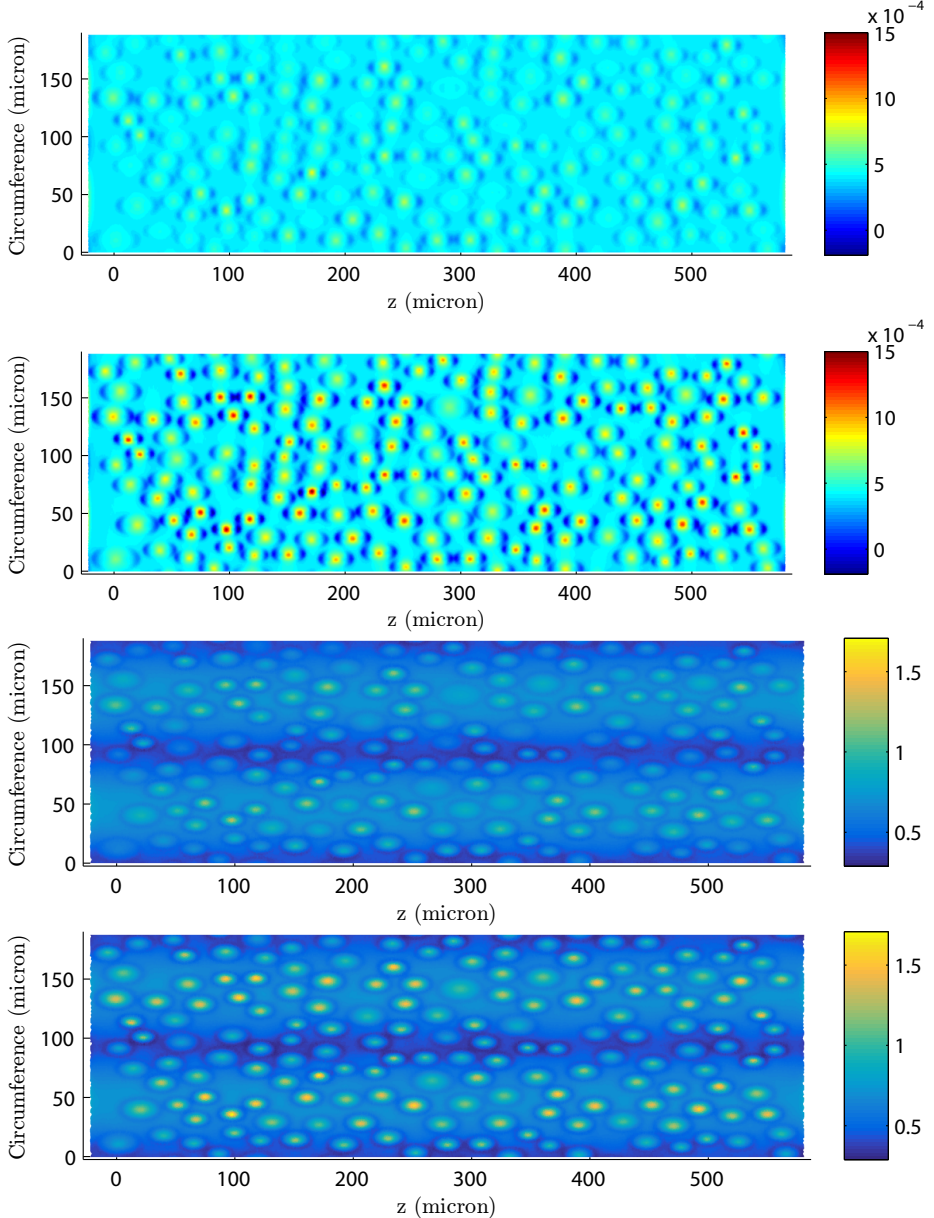


**Figure 7:** Longitudinal component of (a,b) fluid shear stress,  $g_z$ , and (c,d) elastic shear stress,  $h_z$ , exerted upon the endothelium in the low permeability limit ( $K_P = 10^{-12} \text{ cm}^2$ ,  $\lambda = 10^{3.5}$ ) when the minimum EGL thickness is  $t_{\min} = 1.5$ ,  $\alpha_0 = 1.8$ . These stresses are computed using the asymptotic expression (3.10) and (3.27)-(3.29), respectively. We consider both a redistributed EGL of varying thickness (Model A, top image), and a non-redistributed EGL (Model B, bottom image)

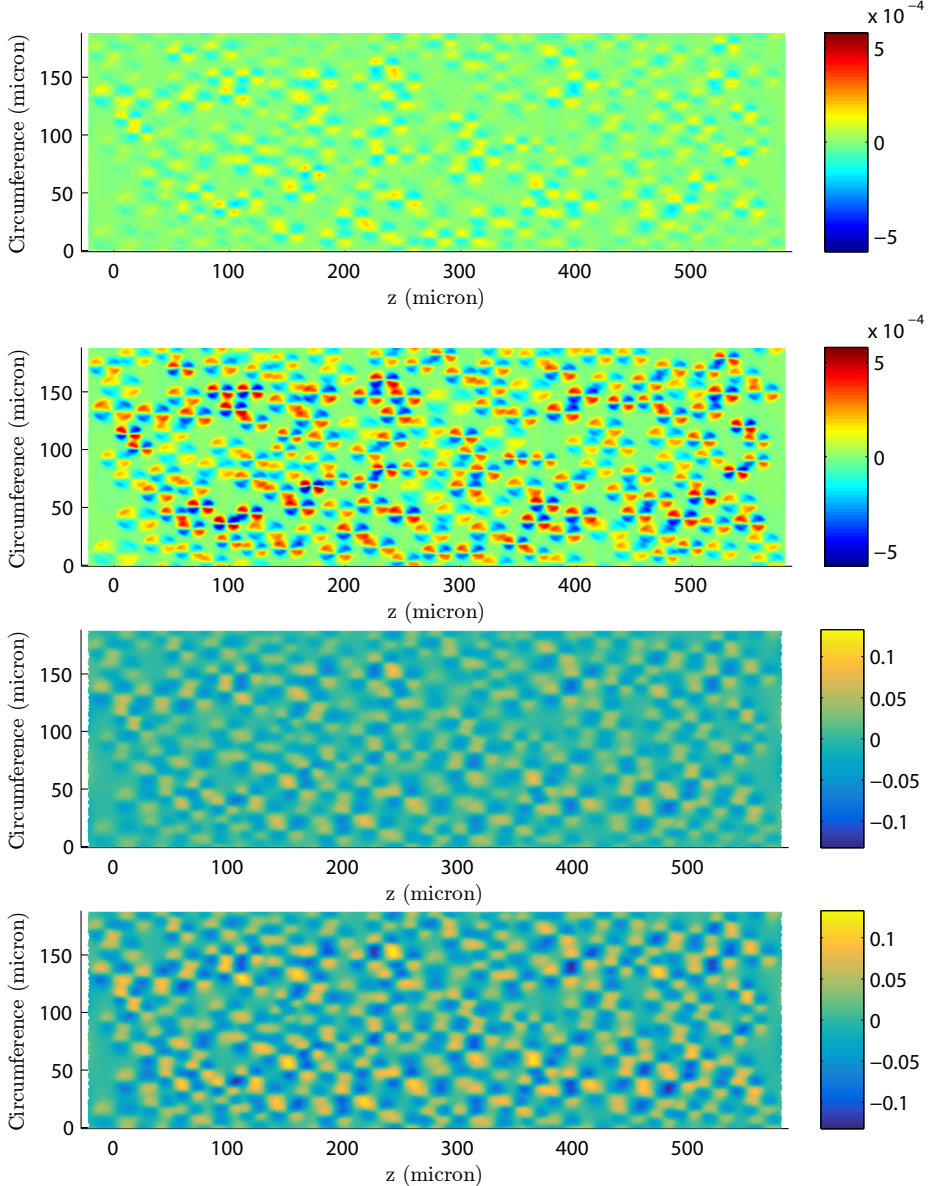


**Figure 8:** Azimuthal component of (a,b) fluid shear stress,  $g_\theta$ , and (c,d) elastic shear stress,  $h_\theta$ , exerted upon the endothelium in the low permeability limit ( $K_P = 10^{-12} \text{ cm}^2$ ,  $\lambda = 10^{3.5}$ ) when the minimum EGL thickness is  $t_{\min} = 1.5$ ,  $\alpha_0 = 1.8$ . These stresses are computed using the asymptotic expression (3.10) and (3.27)-(3.29), respectively. We consider both a redistributed EGL of varying thickness (Model A, top image), and a non-redistributed EGL (Model B, bottom image)

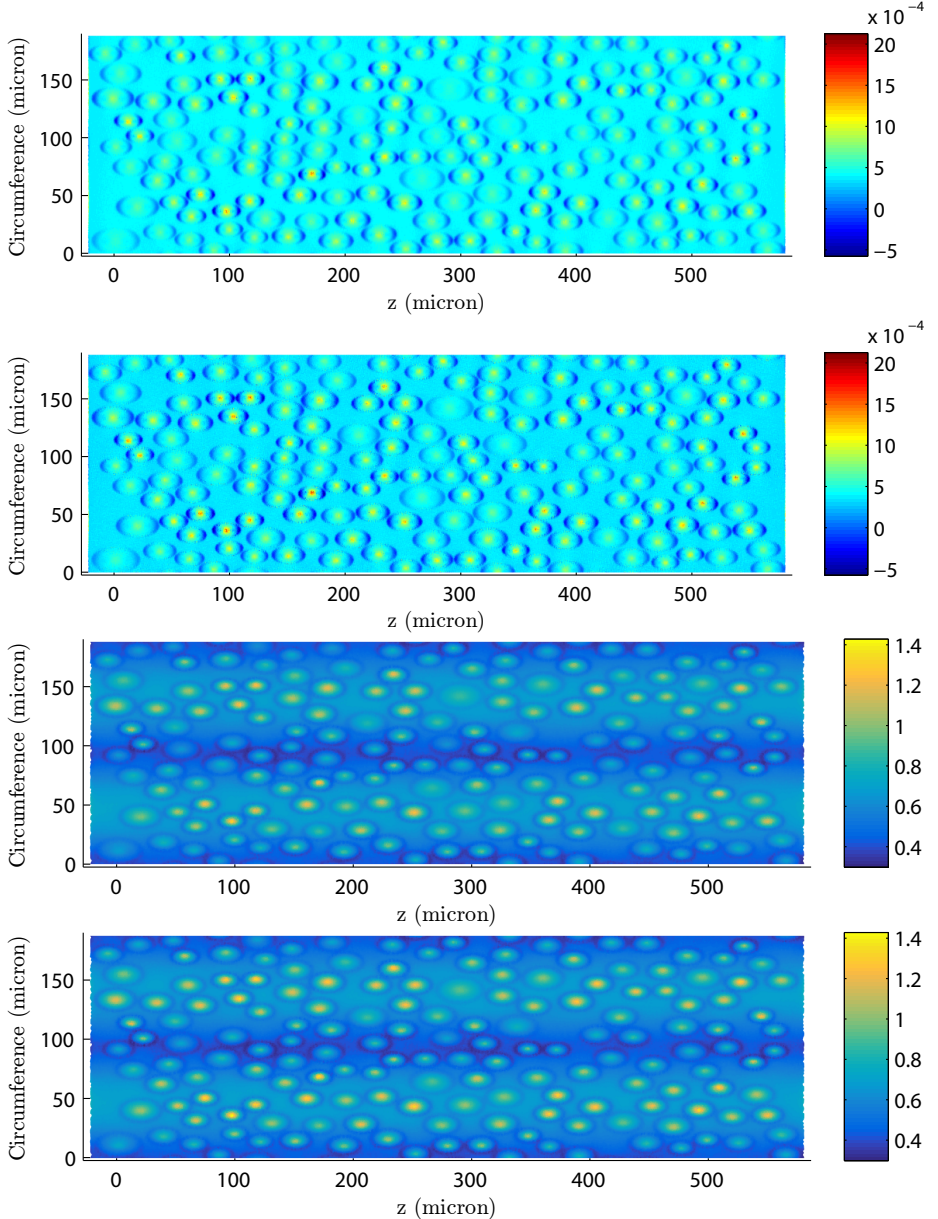


**Figure 9:** Longitudinal component of (a,b) fluid shear stress,  $g_z$ , and (c,d) elastic shear stress,  $h_z$ , exerted upon the endothelium in the low permeability limit ( $K_P = 10^{-12} \text{ cm}^2$ ,  $\lambda = 10^{3.5}$ ) when the minimum EGL thickness is  $t_{\min} = 0.25$ ,  $\alpha_0 = 2.2$ . These stresses are computed using the asymptotic expression (3.10) and (3.27)-(3.29), respectively. We consider both a redistributed EGL of varying thickness (Model A, top image), and a non-redistributed EGL (Model B, bottom image)

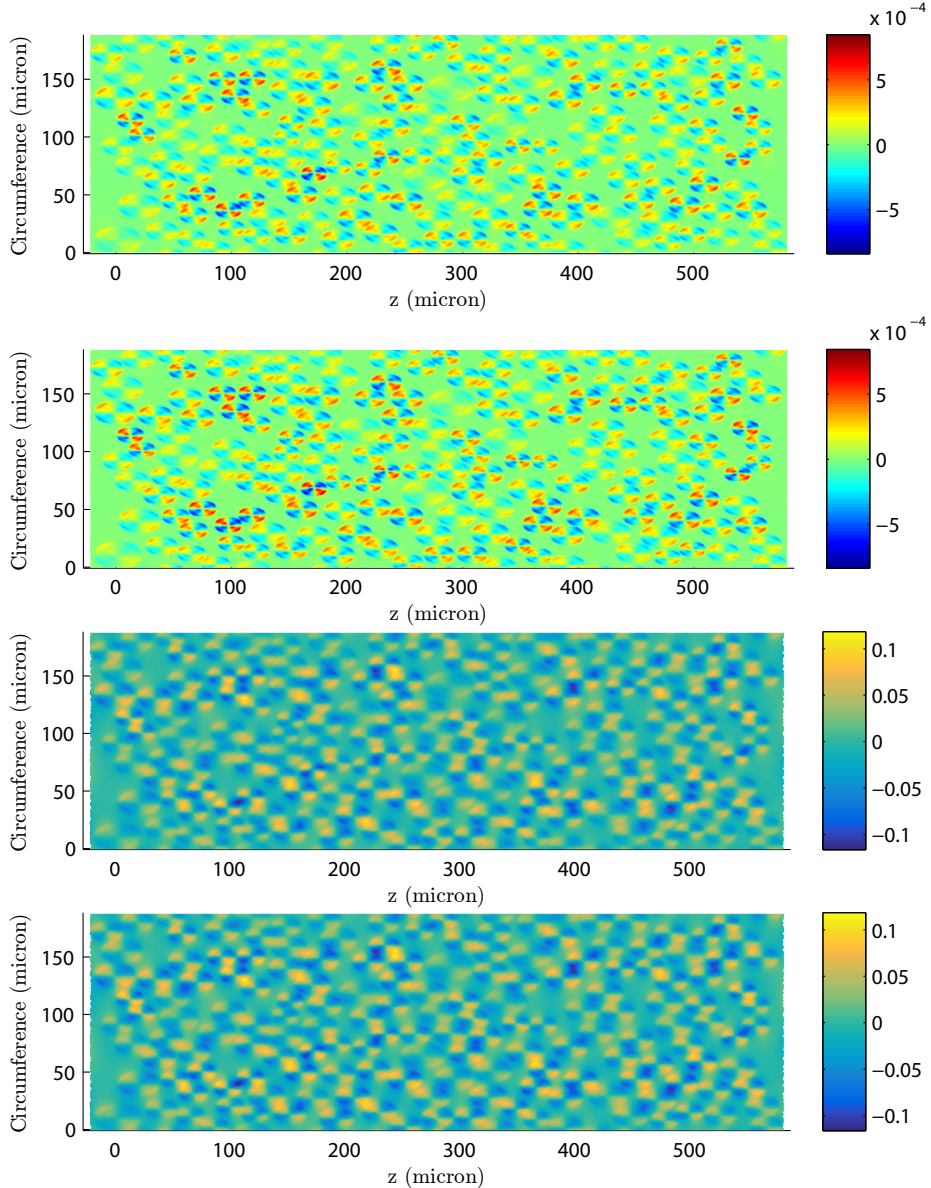


**Figure 10:** Azimuthal component of (a,b) fluid shear stress,  $g_\theta$ , and (c,d) elastic shear stress,  $h_\theta$ , exerted upon the endothelium in the low permeability limit ( $K_P = 10^{-12} \text{ cm}^2$ ,  $\lambda = 10^{3.5}$ ) when the minimum EGL thickness is  $t_{\min} = 0.25$ ,  $\alpha_0 = 2.2$ . These stresses are computed using the asymptotic expression (3.10) and (3.27)-(3.29), respectively. We consider both a redistributed EGL of varying thickness (Model A, top image), and a non-redistributed EGL (Model B, bottom image)

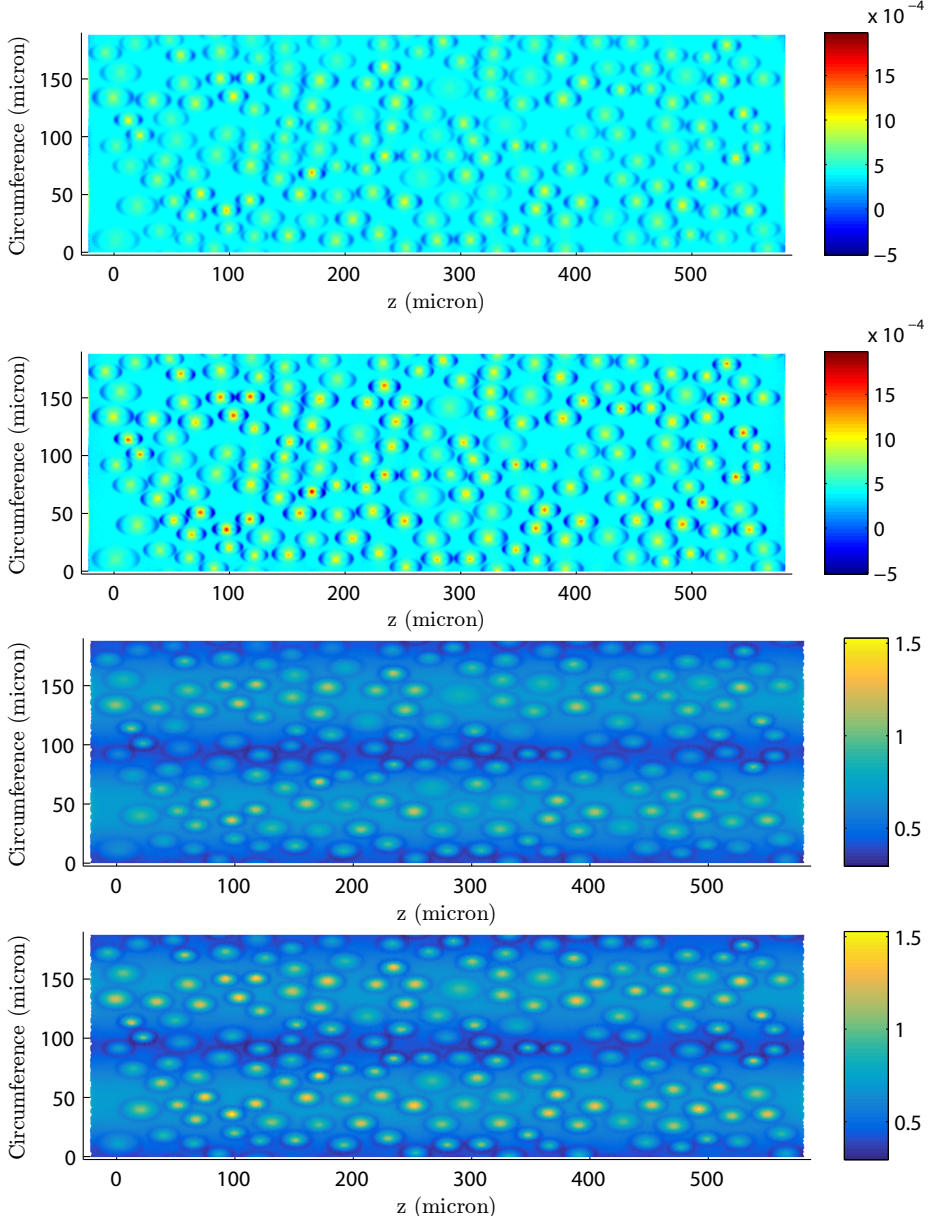


**Figure 11:** Longitudinal component of (a,b) fluid shear stress,  $g_z$ , and (c,d) elastic shear stress,  $h_z$ , exerted upon the endothelium in the low permeability limit ( $K_P = 10^{-12} \text{ cm}^2$ ,  $\lambda = 10^{3.5}$ ) when the minimum EGL thickness is  $t_{\min} = 0.5$ ,  $\alpha_0 = 2.2$ . These stresses are computed using the asymptotic expression (3.10) and (3.27)-(3.29), respectively. We consider both a redistributed EGL of varying thickness (Model A, top image), and a non-redistributed EGL (Model B, bottom image)

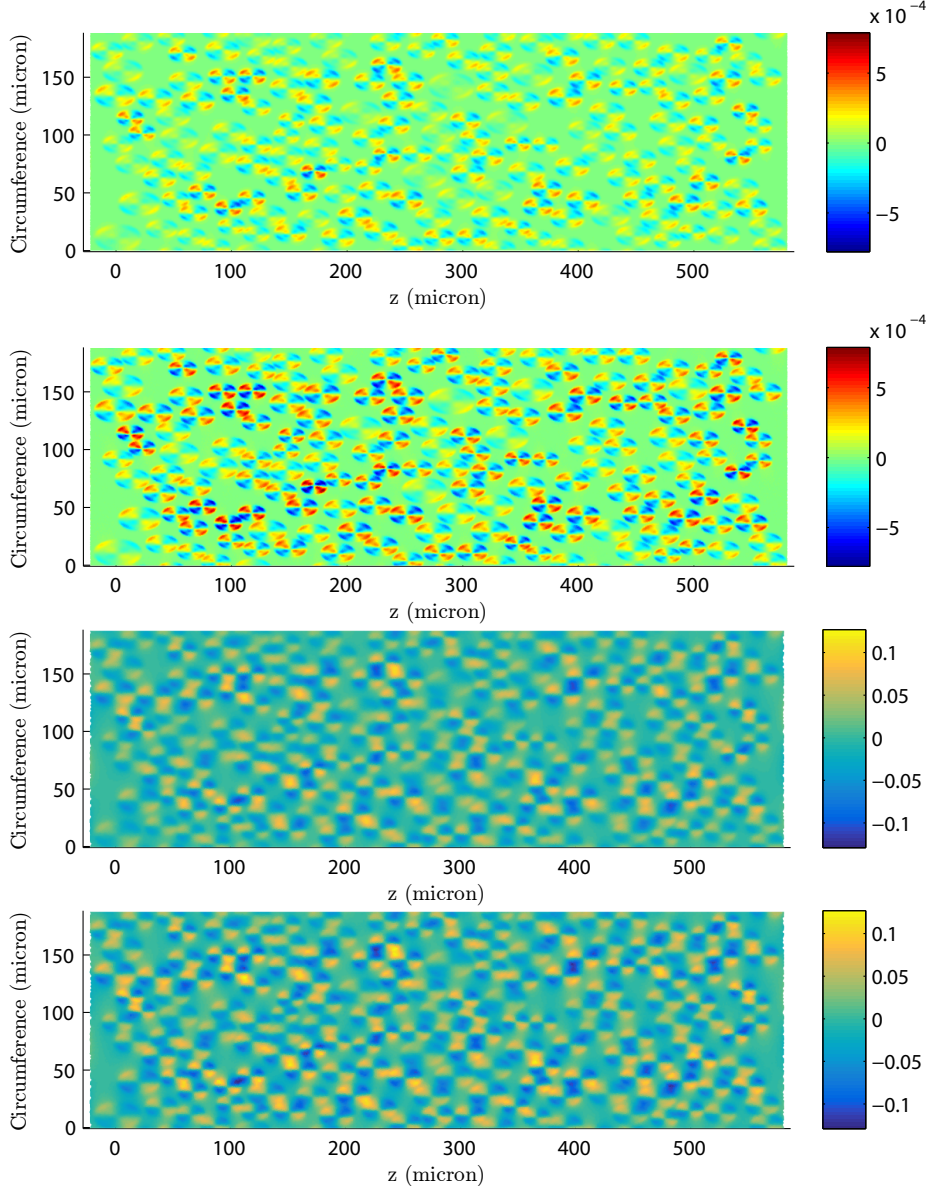


**Figure 12:** Azimuthal component of (a,b) fluid shear stress,  $g_\theta$ , and (c,d) elastic shear stress,  $h_\theta$ , exerted upon the endothelium in the low permeability limit ( $K_P = 10^{-12} \text{ cm}^2$ ,  $\lambda = 10^{3.5}$ ) when the minimum EGL thickness is  $t_{\min} = 0.5$ ,  $\alpha_0 = 2.2$ . These stresses are computed using the asymptotic expression (3.10) and (3.27)-(3.29), respectively. We consider both a redistributed EGL of varying thickness (Model A, top image), and a non-redistributed EGL (Model B, bottom image)

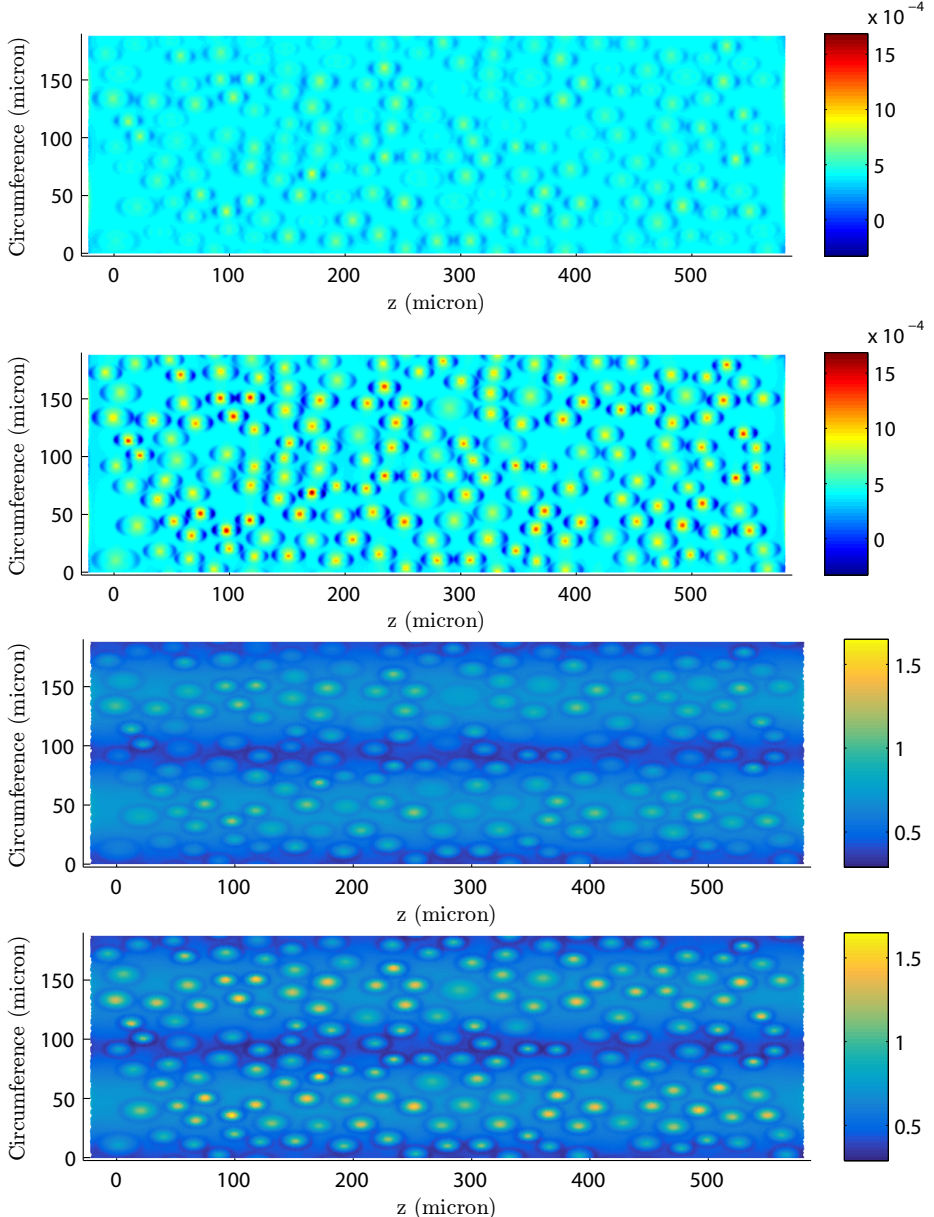


**Figure 13:** Longitudinal component of (a,b) fluid shear stress,  $g_z$ , and (c,d) elastic shear stress,  $h_z$ , exerted upon the endothelium in the low permeability limit ( $K_P = 10^{-12} \text{ cm}^2$ ,  $\lambda = 10^{3.5}$ ) when the minimum EGL thickness is  $t_{\min} = 1$ ,  $\alpha_0 = 2.2$ . These stresses are computed using the asymptotic expression (3.10) and (3.27)-(3.29), respectively. We consider both a redistributed EGL of varying thickness (Model A, top image), and a non-redistributed EGL (Model B, bottom image)

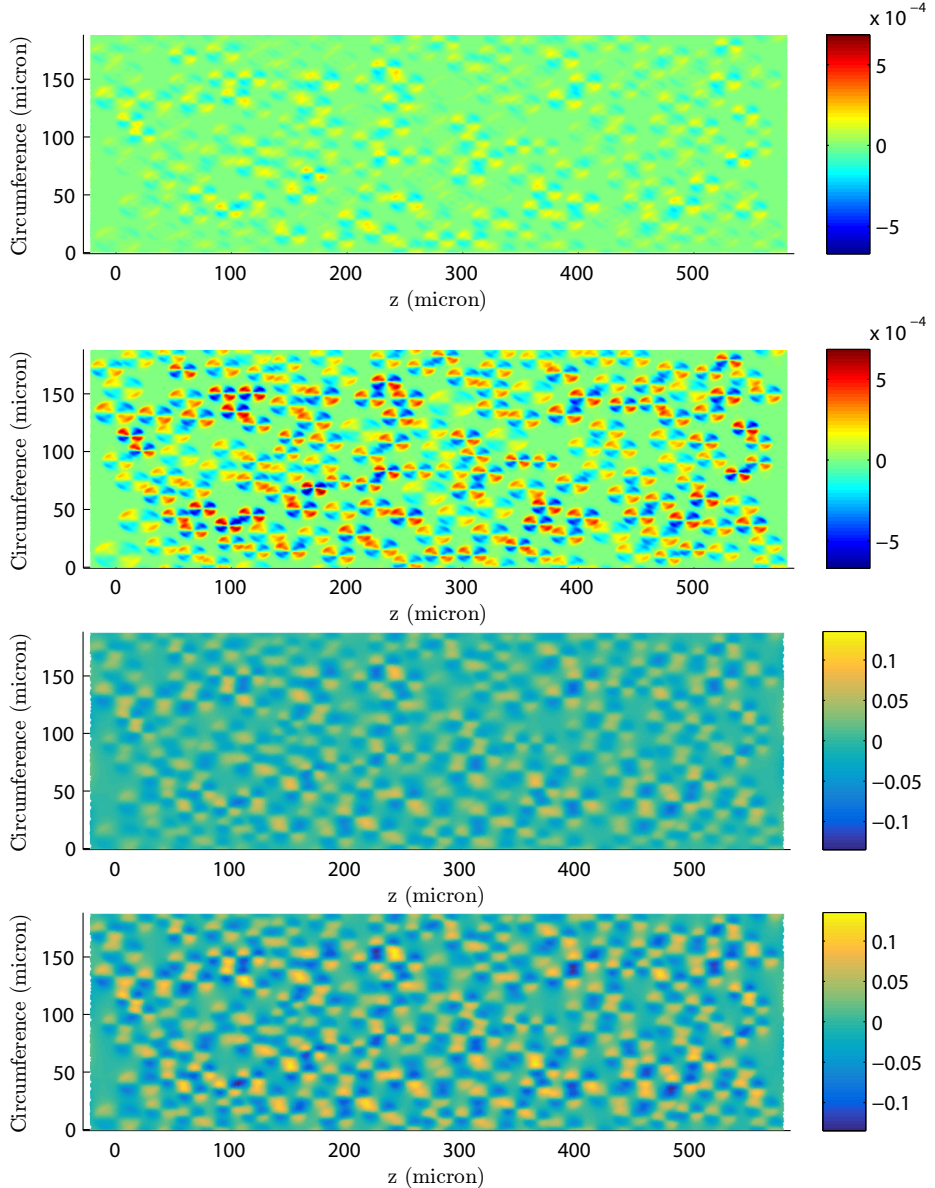


**Figure 14:** Azimuthal component of (a,b) fluid shear stress,  $g_\theta$ , and (c,d) elastic shear stress,  $h_\theta$ , exerted upon the endothelium in the low permeability limit ( $K_P = 10^{-12} \text{ cm}^2$ ,  $\lambda = 10^{3.5}$ ) when the minimum EGL thickness is  $t_{\min} = 1$ ,  $\alpha_0 = 2.2$ . These stresses are computed using the asymptotic expression (3.10) and (3.27)-(3.29), respectively. We consider both a redistributed EGL of varying thickness (Model A, top image), and a non-redistributed EGL (Model B, bottom image)

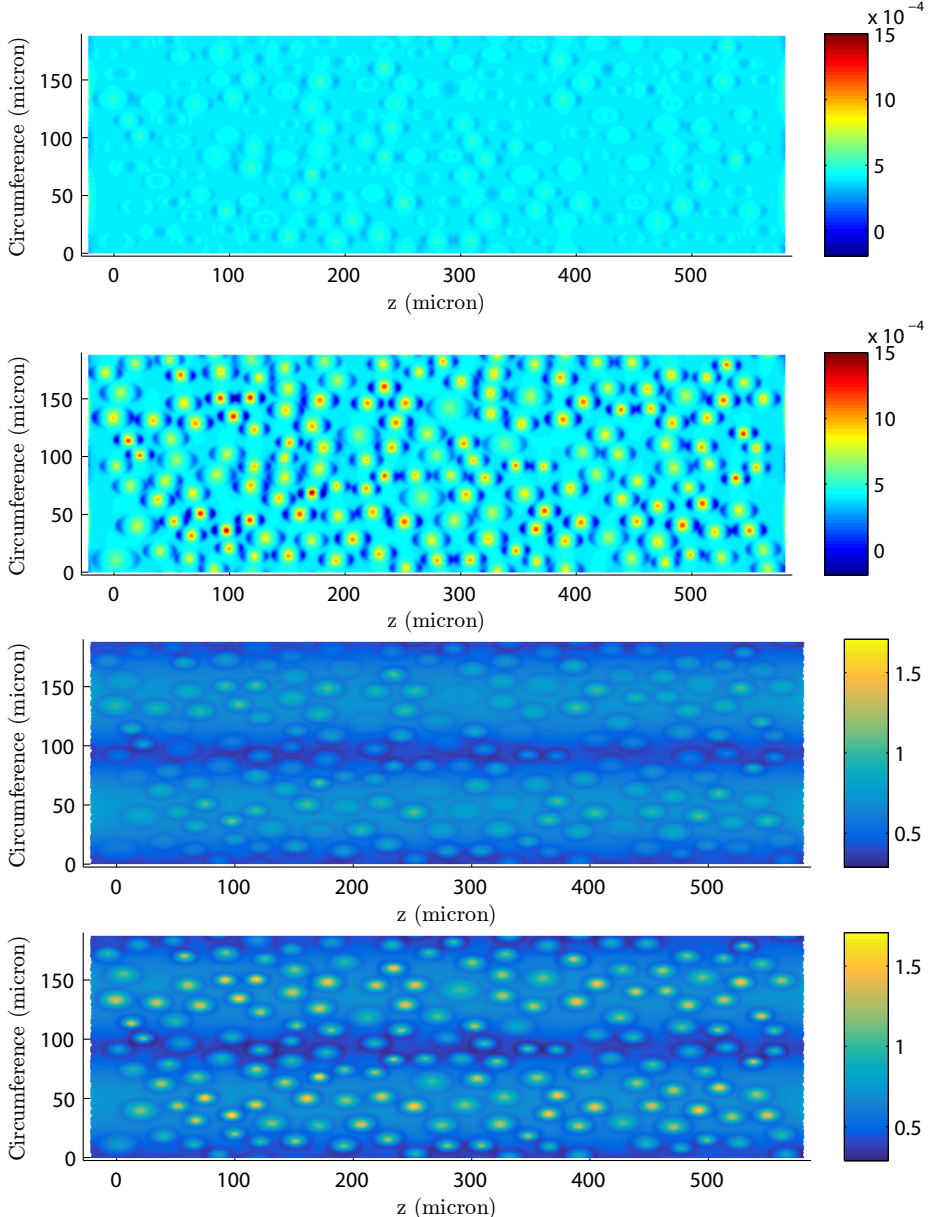


**Figure 15:** Longitudinal component of (a,b) fluid shear stress,  $g_z$ , and (c,d) elastic shear stress,  $h_z$ , exerted upon the endothelium in the low permeability limit ( $K_P = 10^{-12} \text{ cm}^2$ ,  $\lambda = 10^{3.5}$ ) when the minimum EGL thickness is  $t_{\min} = 1.5$ ,  $\alpha_0 = 2.2$ . These stresses are computed using the asymptotic expression (3.10) and (3.27)-(3.29), respectively. We consider both a redistributed EGL of varying thickness (Model A, top image), and a non-redistributed EGL (Model B, bottom image)

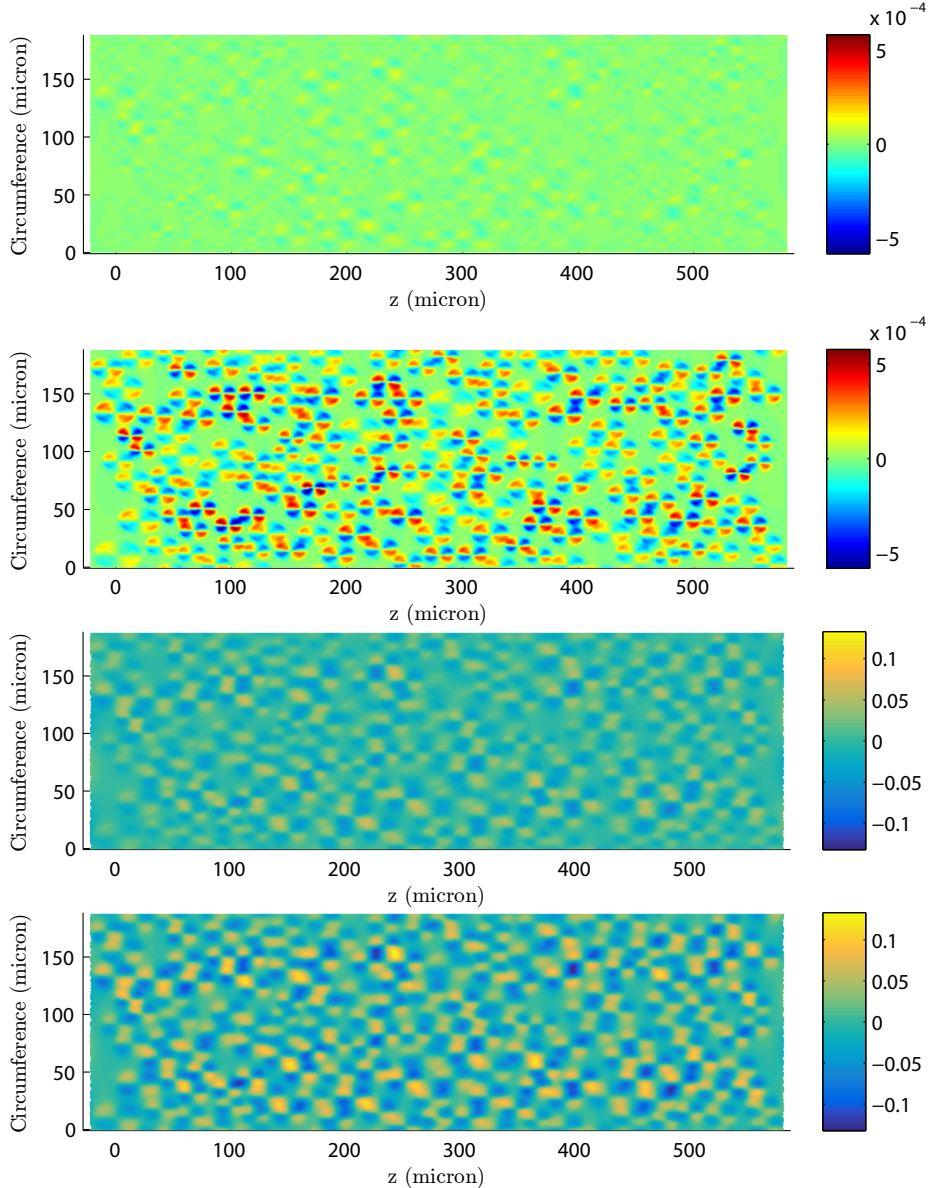


**Figure 16:** Azimuthal component of (a,b) fluid shear stress,  $g_\theta$ , and (c,d) elastic shear stress,  $h_\theta$ , exerted upon the endothelium in the low permeability limit ( $K_P = 10^{-12} \text{ cm}^2$ ,  $\lambda = 10^{3.5}$ ) when the minimum EGL thickness is  $t_{\min} = 1.5$ ,  $\alpha_0 = 2.2$ . These stresses are computed using the asymptotic expression (3.10) and (3.27)-(3.29), respectively. We consider both a redistributed EGL of varying thickness (Model A, top image), and a non-redistributed EGL (Model B, bottom image)

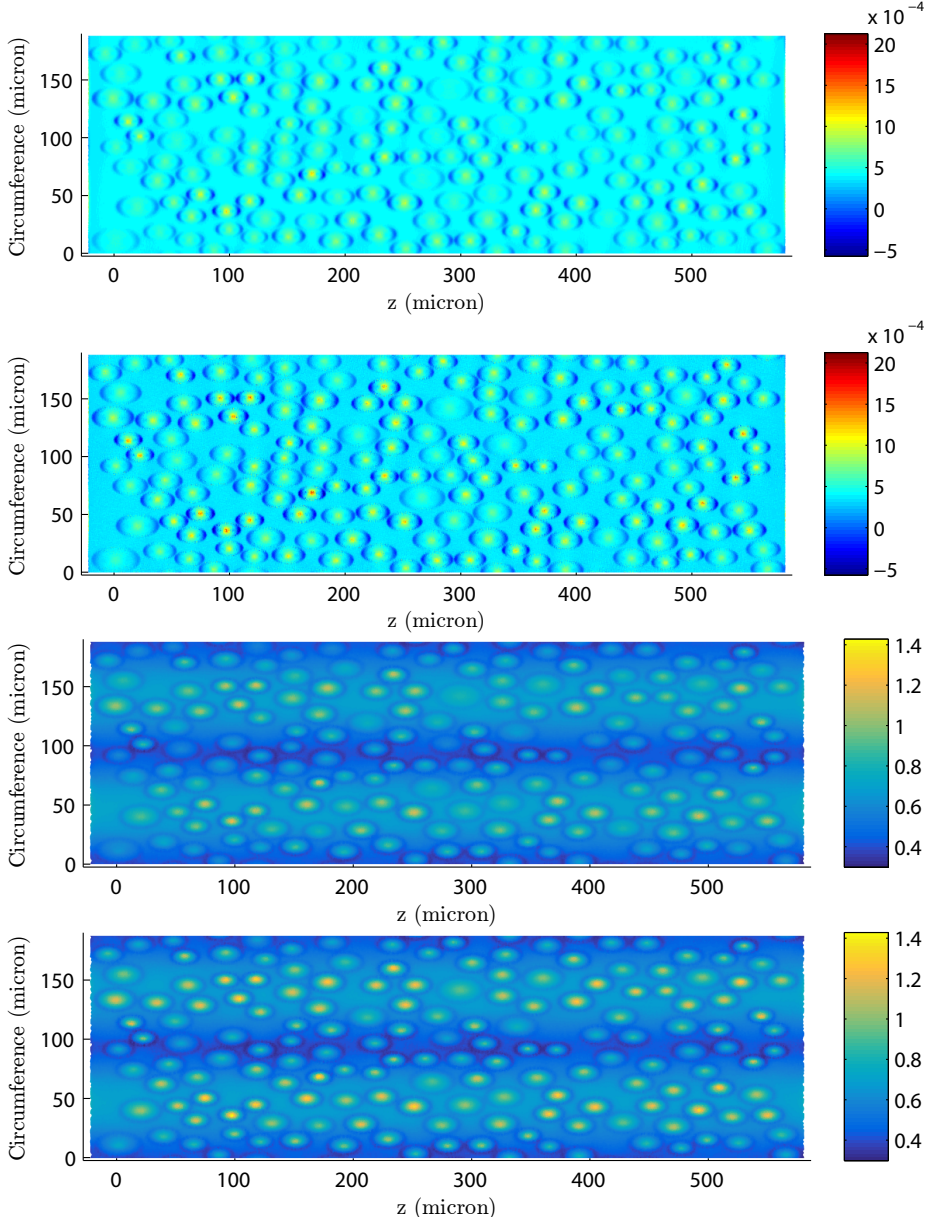


**Figure 17:** Longitudinal component of (a,b) fluid shear stress,  $g_z$ , and (c,d) elastic shear stress,  $h_z$ , exerted upon the endothelium in the low permeability limit ( $K_P = 10^{-12} \text{ cm}^2$ ,  $\lambda = 10^{3.5}$ ) when the minimum EGL thickness is  $t_{\min} = 0.25$ ,  $\alpha_0 = 3.4$ . These stresses are computed using the asymptotic expression (3.10) and (3.27)-(3.29), respectively. We consider both a redistributed EGL of varying thickness (Model A, top image), and a non-redistributed EGL (Model B, bottom image)

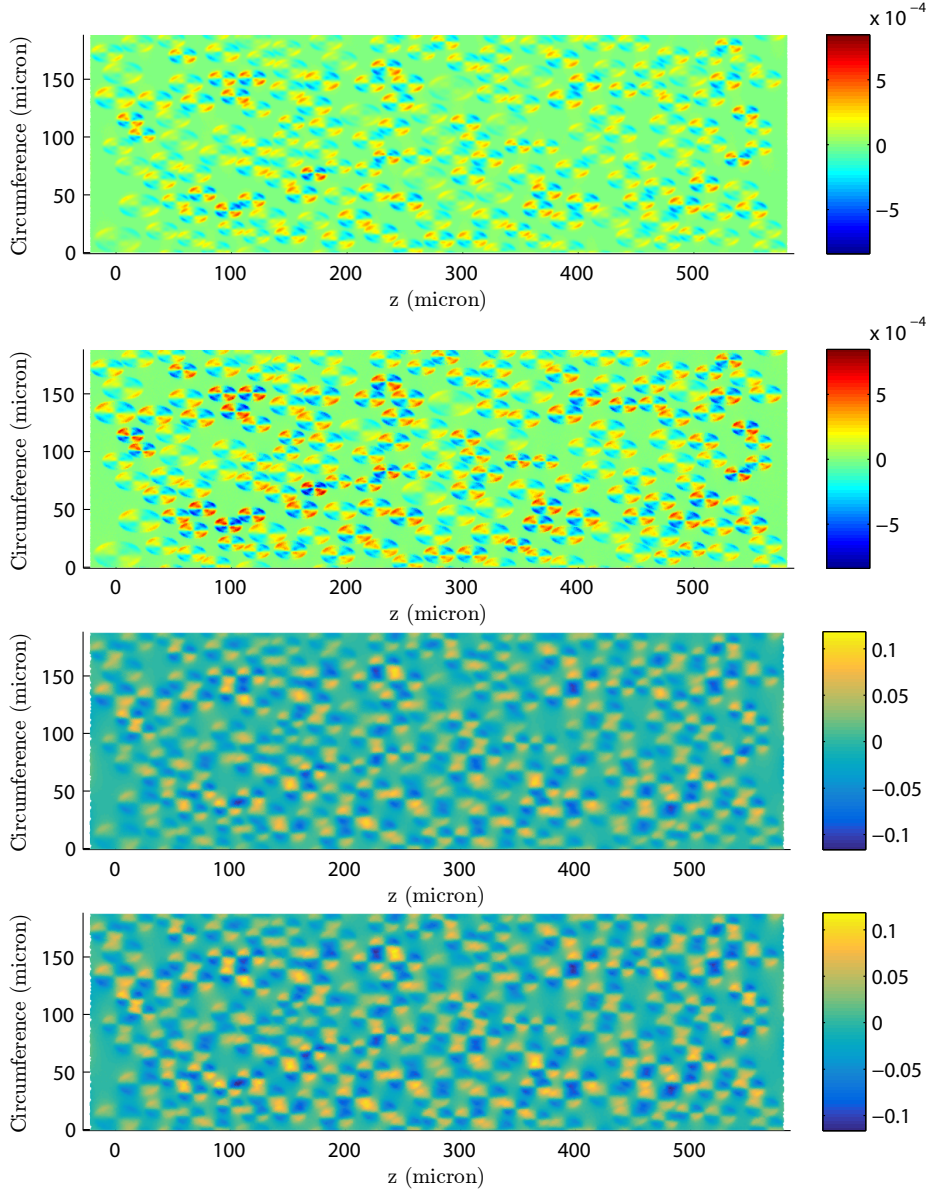


**Figure 18:** Azimuthal component of (a,b) fluid shear stress,  $g_\theta$ , and (c,d) elastic shear stress,  $h_\theta$ , exerted upon the endothelium in the low permeability limit ( $K_P = 10^{-12} \text{ cm}^2$ ,  $\lambda = 10^{3.5}$ ) when the minimum EGL thickness is  $t_{\min} = 0.25$ ,  $\alpha_0 = 3.4$ . These stresses are computed using the asymptotic expression (3.10) and (3.27)-(3.29), respectively. We consider both a redistributed EGL of varying thickness (Model A, top image), and a non-redistributed EGL (Model B, bottom image)

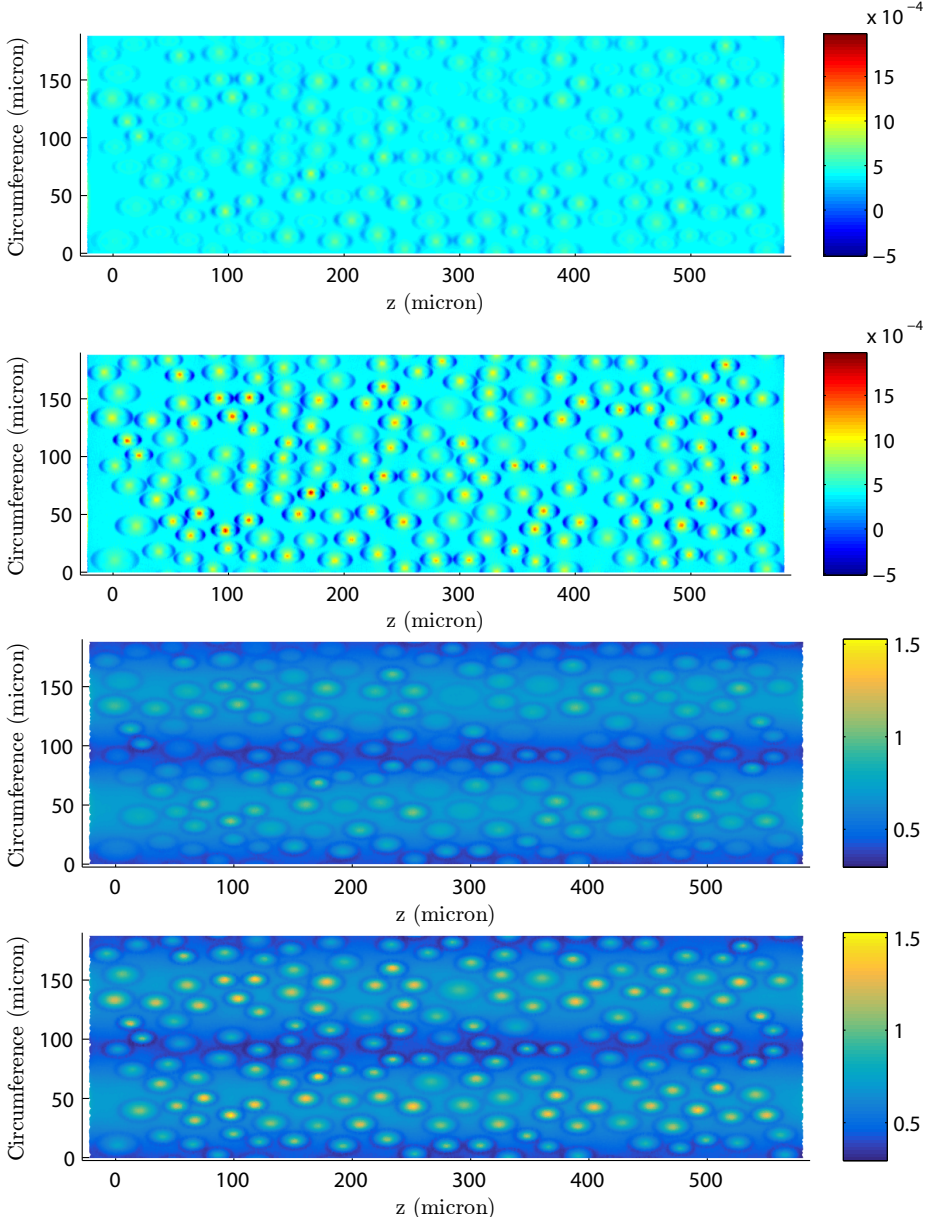


**Figure 19:** Longitudinal component of (a,b) fluid shear stress,  $g_z$ , and (c,d) elastic shear stress,  $h_z$ , exerted upon the endothelium in the low permeability limit ( $K_P = 10^{-12} \text{ cm}^2$ ,  $\lambda = 10^{3.5}$ ) when the minimum EGL thickness is  $t_{\min} = 0.5$ ,  $\alpha_0 = 3.4$ . These stresses are computed using the asymptotic expression (3.10) and (3.27)-(3.29), respectively. We consider both a redistributed EGL of varying thickness (Model A, top image), and a non-redistributed EGL (Model B, bottom image)

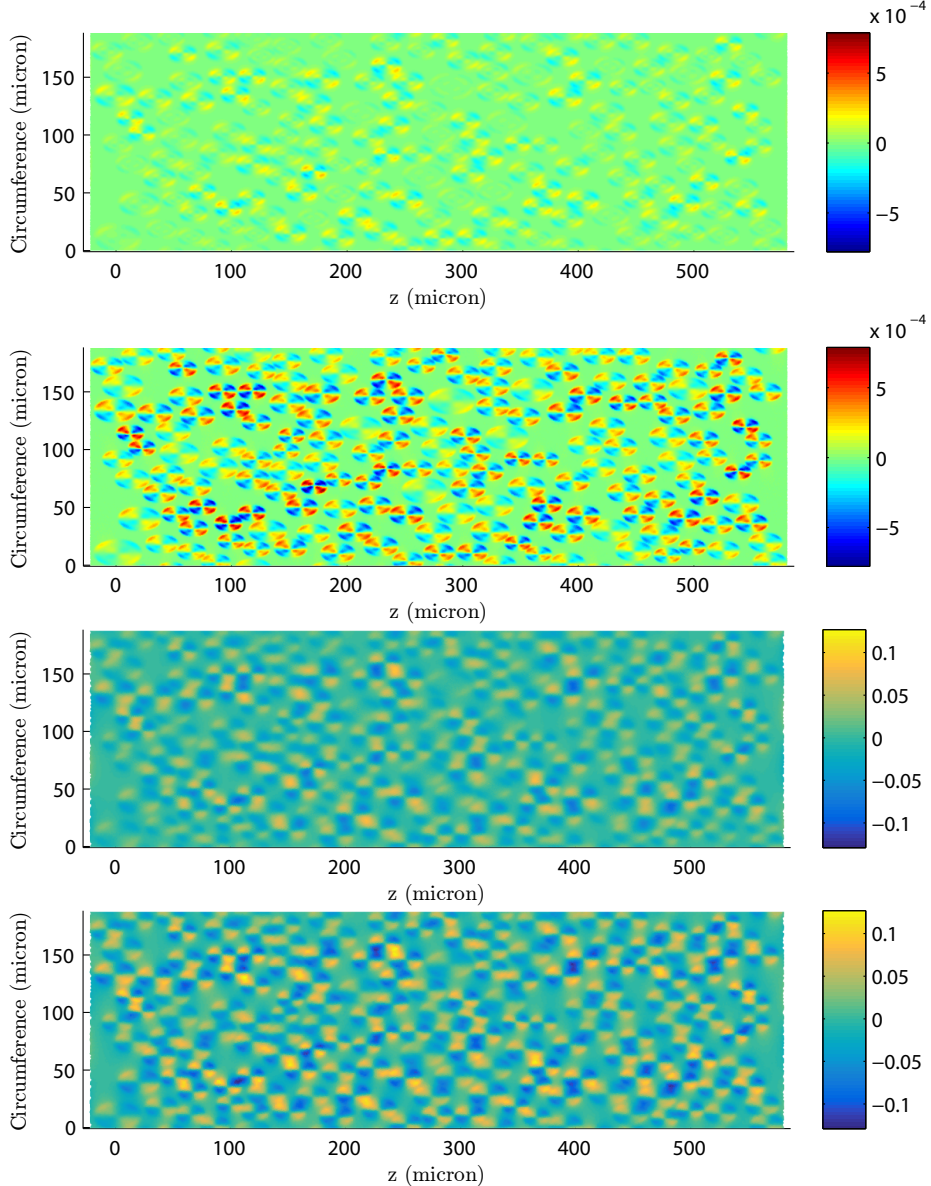


**Figure 20:** Azimuthal component of (a,b) fluid shear stress,  $g_\theta$ , and (c,d) elastic shear stress,  $h_\theta$ , exerted upon the endothelium in the low permeability limit ( $K_P = 10^{-12} \text{ cm}^2$ ,  $\lambda = 10^{3.5}$ ) when the minimum EGL thickness is  $t_{\min} = 0.5$ ,  $\alpha_0 = 3.4$ . These stresses are computed using the asymptotic expression (3.10) and (3.27)-(3.29), respectively. We consider both a redistributed EGL of varying thickness (Model A, top image), and a non-redistributed EGL (Model B, bottom image)

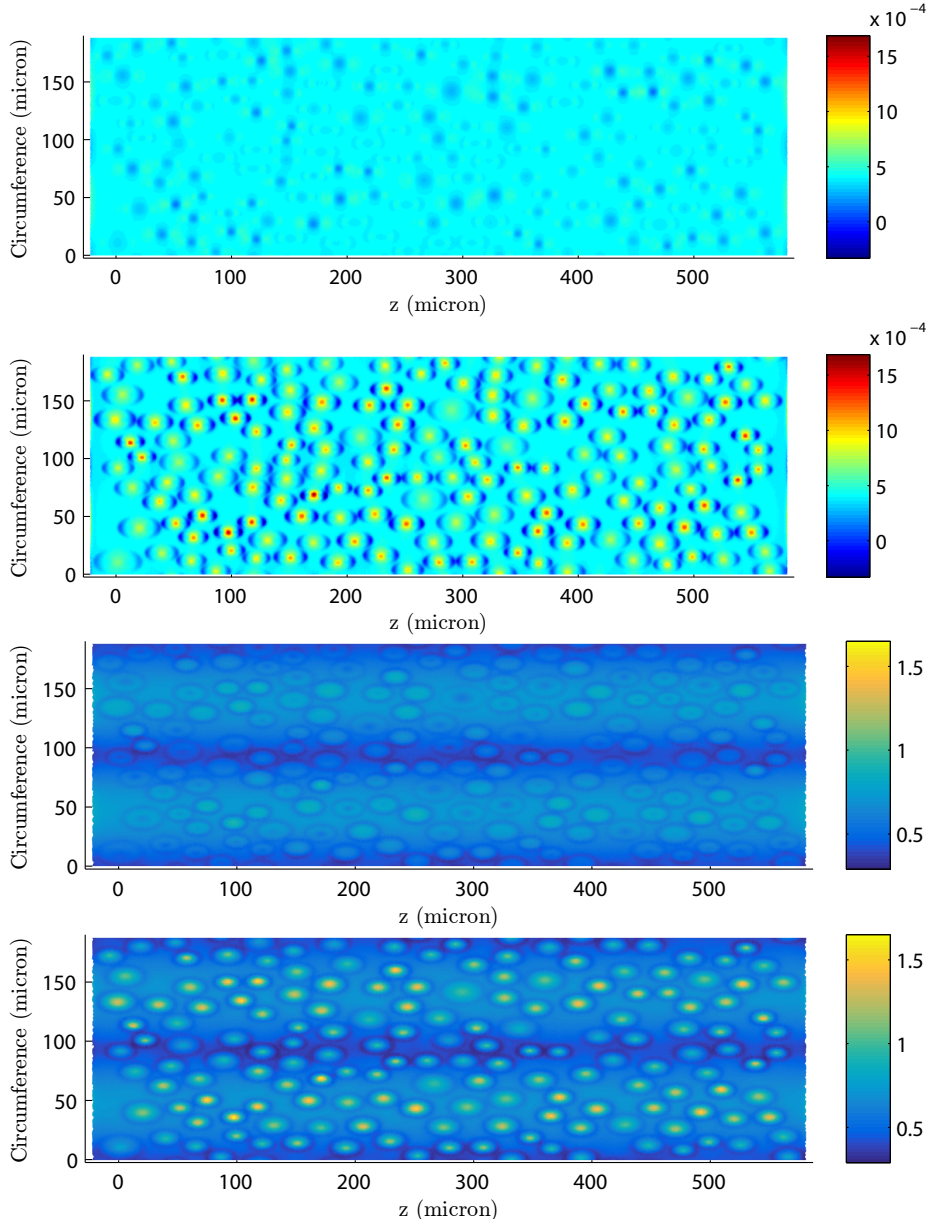


**Figure 21:** Longitudinal component of (a,b) fluid shear stress,  $g_z$ , and (c,d) elastic shear stress,  $h_z$ , exerted upon the endothelium in the low permeability limit ( $K_P = 10^{-12} \text{ cm}^2$ ,  $\lambda = 10^{3.5}$ ) when the minimum EGL thickness is  $t_{\min} = 1$ ,  $\alpha_0 = 3.4$ . These stresses are computed using the asymptotic expression (3.10) and (3.27)-(3.29), respectively. We consider both a redistributed EGL of varying thickness (Model A, top image), and a non-redistributed EGL (Model B, bottom image)

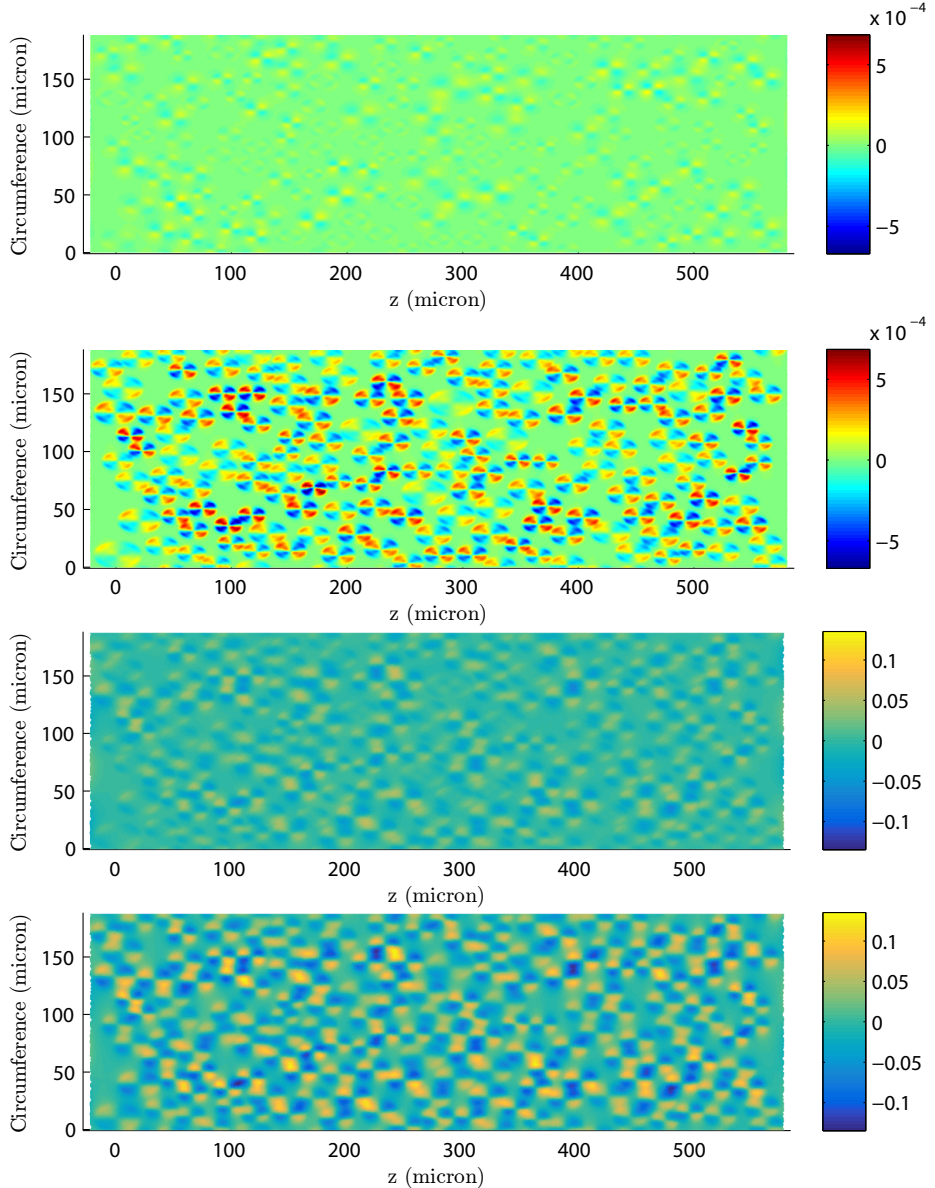


**Figure 22:** Azimuthal component of (a,b) fluid shear stress,  $g_\theta$ , and (c,d) elastic shear stress,  $h_\theta$ , exerted upon the endothelium in the low permeability limit ( $K_P = 10^{-12} \text{ cm}^2$ ,  $\lambda = 10^{3.5}$ ) when the minimum EGL thickness is  $t_{\min} = 1$ ,  $\alpha_0 = 3.4$ . These stresses are computed using the asymptotic expression (3.10) and (3.27)-(3.29), respectively. We consider both a redistributed EGL of varying thickness (Model A, top image), and a non-redistributed EGL (Model B, bottom image)

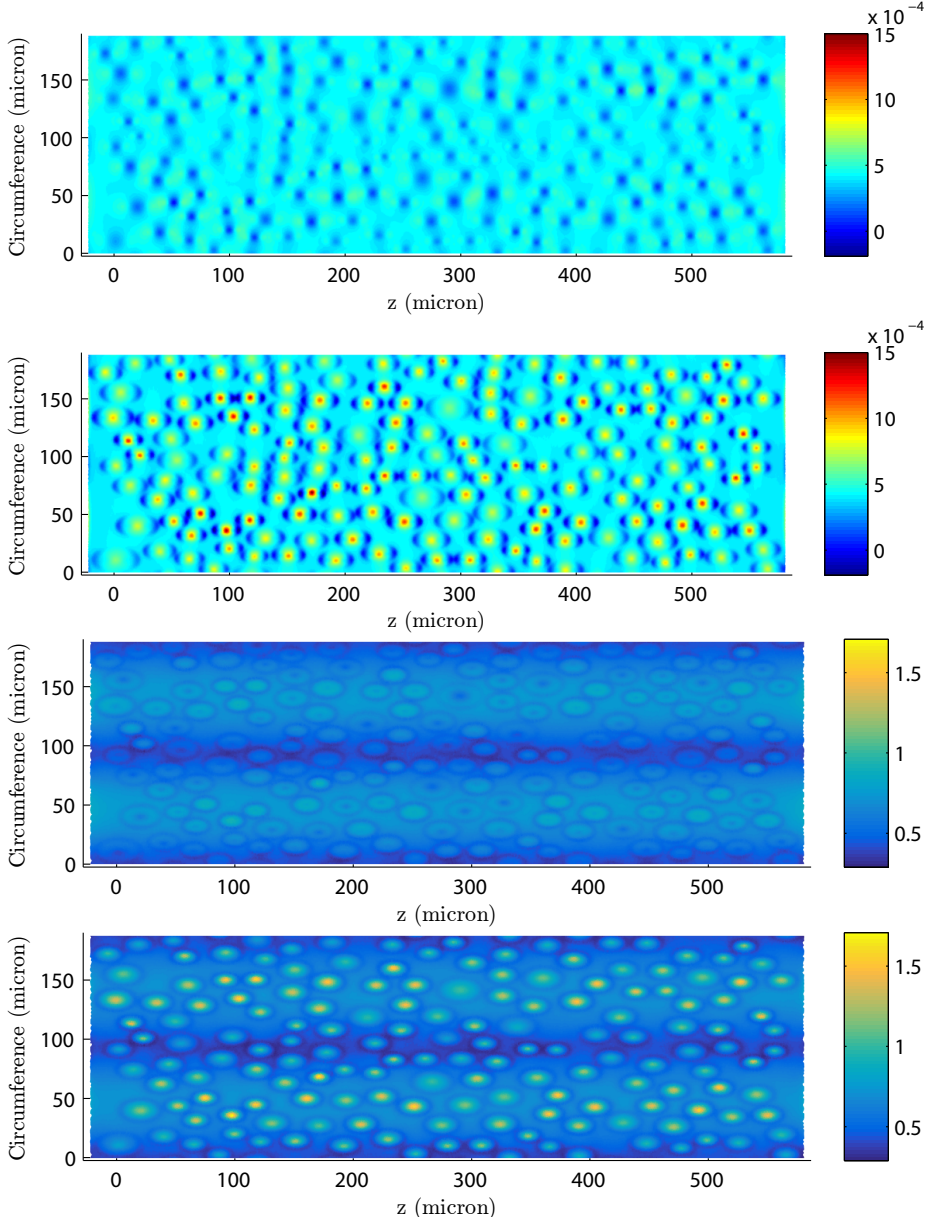


**Figure 23:** Longitudinal component of (a,b) fluid shear stress,  $g_z$ , and (c,d) elastic shear stress,  $h_z$ , exerted upon the endothelium in the low permeability limit ( $K_P = 10^{-12} \text{ cm}^2$ ,  $\lambda = 10^{3.5}$ ) when the minimum EGL thickness is  $t_{\min} = 1.5$ ,  $\alpha_0 = 3.4$ . These stresses are computed using the asymptotic expression (3.10) and (3.27)-(3.29), respectively. We consider both a redistributed EGL of varying thickness (Model A, top image), and a non-redistributed EGL (Model B, bottom image)

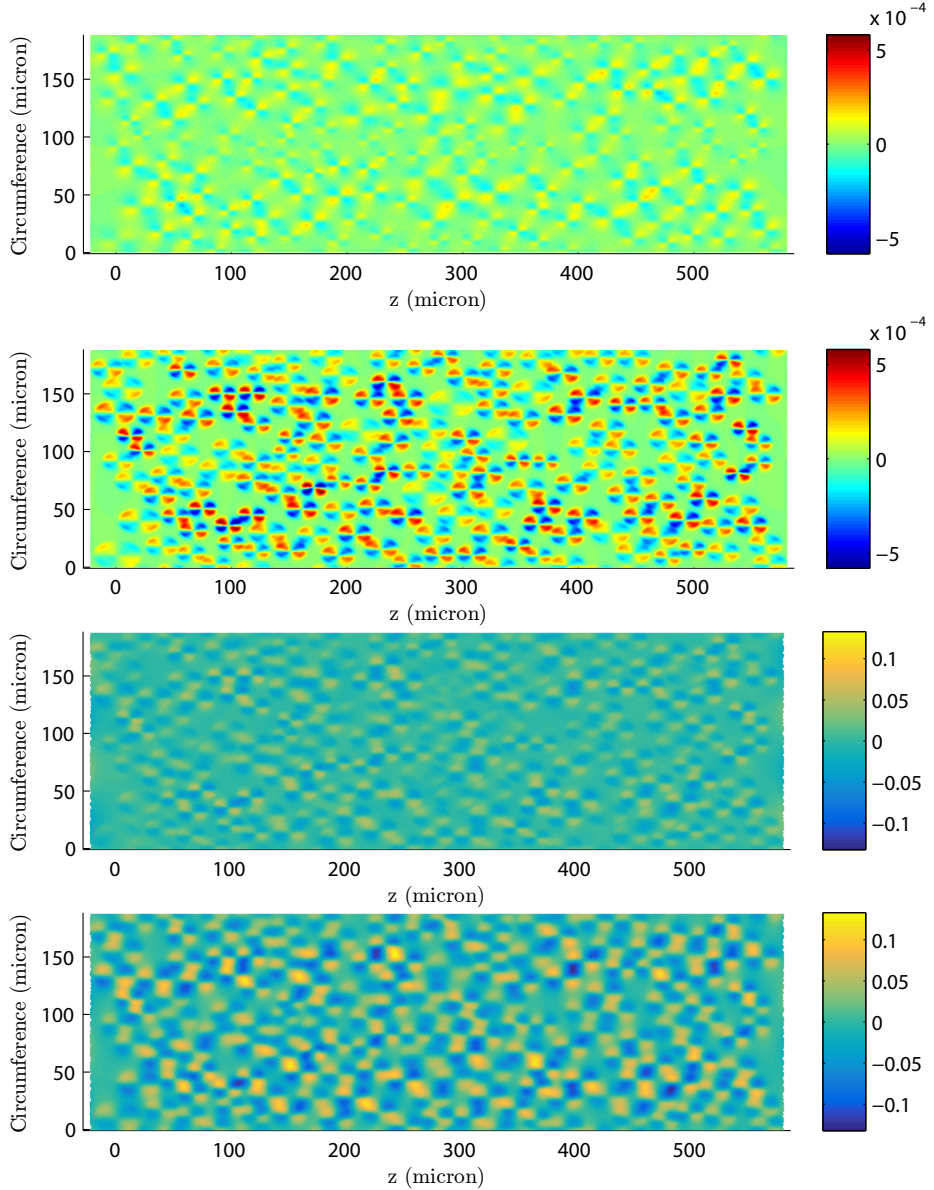


**Figure 24:** Azimuthal component of (a,b) fluid shear stress,  $g_\theta$ , and (c,d) elastic shear stress,  $h_\theta$ , exerted upon the endothelium in the low permeability limit ( $K_P = 10^{-12} \text{ cm}^2$ ,  $\lambda = 10^{3.5}$ ) when the minimum EGL thickness is  $t_{\min} = 1.5$ ,  $\alpha_0 = 3.4$ . These stresses are computed using the asymptotic expression (3.10) and (3.27)-(3.29), respectively. We consider both a redistributed EGL of varying thickness (Model A, top image), and a non-redistributed EGL (Model B, bottom image)